Open Poster Session

SOME OBSERVATIONS ON THE PERFORMANCE OF MODERN WIDEBAND CURRENT TRANSFORMERS IN PULSE CURRENT MEASUREMENT APPLICATIONS

*B.V. Cordingley and D.J. Chamund**
Lilco Ltd, Livingston, U.K., *Dynex Semiconductor, Lincoln, U.K.

Abstract
In this paper the analysis of the performance of both internally- and externally-terminated current transformers (ct's) is presented. Factors limiting the I-t, droop, peak pulse current, frequency response and mean dc current performance of these instruments are discussed and the trade-offs examined. Experimental results which demonstrate the behaviour of inexpensive ring-type designs over a broad spectrum of frequencies are examined and compared with those achieved with internally-terminated structures. It is shown that some unterminated ring-type designs can produce a good and versatile performance in the measurement of pulse currents with frequency components below 0.1Hz and to several 100kHz. Internally-terminated designs extend the performance by two to three decades of frequency for applications where high-frequency harmonics are to be measured accurately.

INTRODUCTION

Terminated current transformers have been used to measure pulse currents in power electronics for several decades. Arguably their greatest attribute is that they permit the measurement of current without the need for direct electrical connection to the circuit under test. This quality greatly facilitates the concurrent measurement of other electrical parameters [1]. These instruments can record currents measured in milliamps to pulse currents of several hundred thousand amps whilst imposing little burden on the system under test. Terminated current transformers combine this broad dynamic range with an impressive bandwidth. There are commercially-available instruments that can measure pulse currents with harmonic components in the range 0.1Hz to 100MHz. They have the ability to replicate a high-current waveshape with good fidelity for capture by a data recorder or display on an oscilloscope. Indeed, where the highest frequency components are to be measured it is difficult to envisage an alternative system of measurement.

The performance of a ct is governed in some measure by the properties of the magnetic materials employed in its construction. For the magnetic circuit, the strip-wound toroidal structure is preferred. Materials used in commercial products include grain-orientated steel (GOS), nickel-iron alloys such as mumetal and, more recently, nanocrystalline and amorphous iron alloys. Some of the properties of these materials are examined and compared in this contribution.

In pulse applications, both low-frequency characteristics, such as I-t capability and droop performance, and high-frequency characteristics, such as rise-time and stray signal pick up, are important. In this paper we employ the appropriate equivalent circuits to explore the nature these characteristics.

The construction of transformers designed for the measurement of the high-frequency components in very high current pulses can cause some difficulties to the transformer manufacturer. In the latter part of this paper we illustrate how characteristics of cascaded

transformers can be combined to produce a high-frequency performance that is difficult to match in a single instrument.

EQUIVALENT CIRCUITS

In analysing the performance of a broadband current transformer it is convenient to refer to both the low-frequency and high-frequency transformer equivalent circuits.

Low-frequency equivalent circuit

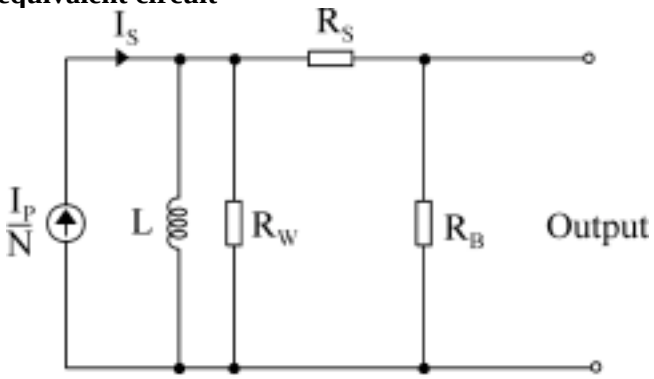

Fig.1 Low-frequency equivalent circuit

In Fig. 1

I_s is the secondary current. This is essentially a constant current equal to I_p/N where N is the transformer turns ratio and I_p the primary current

L is the inductance of the secondary winding,

R_W is the core watts loss,

R_s is the resistance of the secondary winding and

R_B is the burden or sense resistor.

The instrument is essentially a transducer which converts primary current to a voltage signal. Its sensitivity is equal to R_B/N volts per primary amp. In transformers designed for pulse measurement, R_W can be made sufficiently small for it to be ignored. It can be seen, that for faithful reproduction of the primary current waveform, the current flowing in L must be significantly less that that flowing in R_s and R_B. The low frequency 3dB cut-off point f_{lfco} is given by:

$$f_{lfco} \cong (R_W + R_B)/2\pi L \quad (1)$$

Where $$L=(\mu_r\mu_0 N_s^2 A_{fe})/l_{fe} \quad (2)$$

μ_r is the relative permeability of the core material,
μ_0 is the permeability of free space,
N_s the number of secondary turns which is equal to N when, as often is the case, a single-turn primary is employed,
A_{fe} is the effective area of cross section of the core and
L_{fe} is the mean length of the magnetic path.

The ability of the instrument to display a rectangular waveform without saturation is known as I-t capability. It is given by:

$$I\text{-}t \cong (B_s A_{fe} Ns^2)/(R_W + R_B) \quad (3)$$

Where B_s is the saturation flux density for the core material. This equation is valid where droop is small over the period of the pulse. See Refs [2] and [3].

When a rectangular waveform is measured the output signal deviates from the true value with time. This deviation or droop is caused by the increase in the current flowing into L in the presence of a constant output voltage. It can be shown that

$$\text{Droop} = 0.1(R_s + R_B)/L \ \%/\text{ms} \quad (4)$$

Droop is a measure of the rate of exponential decay of the recorded value of current from its true value. The flow of current in L also results in a phase shift between input and output signals. For more information on this and droop see Ref [3].

In some pulsed applications there can be a significant dc component of current present. The primary dc current that can saturate the transformers core can be found from

$$I_p = B_s I_{fe}/\mu_r \mu_0 \quad (5)$$

Though this relationship is for guidance only as μ_r is often a strong function of flux density.

High-frequency equivalent circuit

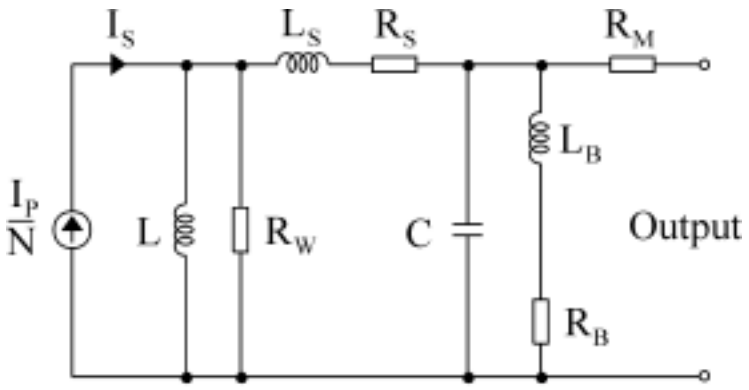

Fig. 2 High-frequency equivalent circuit

At high frequency, parasitic inductance and capacitance limits the performance of the transformer.

L_s represents the parasitic inductance caused by leakage flux.

C represents the parasitic capacitance.

L_B is the parasitic series inductance associated with the sense resistor.

R_M is the resistor used to match the output impedance of the instrument to its connecting cable.

The positioning of the capacitance C in Fig. 2 is more symbolic than to assist with analysis. It represents the distributed stray winding-to-winding, winding-to-shield and winding-to-core capacitances.

Unlike low-frequency characteristics which lend themselves to determination by calculation, the high-frequency design depends more on the experience of the designer. For internally-terminated transformers the effect of stay inductance and capacitance is reduced by essentially constructing multiple series-connected transformers to form a single unit. By this means pulse power transformers can be constructed with a high-frequency cut-off point that is beyond 100MHz.

Factors can limit effective high-frequency performance include:

(1) The stray inductive and capacitive components can cause oscillation, attenuation or overshoot of the output at a limiting frequency.

(2) Loss of core permeability at high frequency can make the instrument over-sensitive to magnetic pick up.

(3) The stray inductance, L_B associated with resistor R_B, can cause distortion of the output signal. For high pulse currents, a low-sensitivity and high I-t capability are required. These attributes are achieved in part by selecting a low value for R_B. L_B tends to have a constant value for a particular resistor design and its inductive reactance can limit hf performance as its value approaches that of R_B. Ironically, the employment of multiple stages in internally-terminated transformers tends to exacerbate the problem as effectively the total value of R_B has to be achieved by the series connection of several discrete resistors each with its associated L_B. The cascade arrangement illustrated later in this paper can mitigate this limitation.

MAGNETIC PROPERTIES OF SOME STRIP-WOUND MATERIALS

The lowest-cost core material suited for pulse transformer core manufacture is grain orientated silicon steel. Its cost makes its use attractive where a large volume of core material is required. Other materials that are used include Ni-Fe alloys and modern materials such as nanocrystalline iron alloys. The latter material is somewhat more expensive than the former though its magnetic properties can often justify the price differential. In Figs 3 and 4 curves illustrating two important magnetic properties of these materials with regard to their use in wideband current transformers are illustrated. The curves are for M4 grade GOS, the Ni-Fe alloy mumetal and a high-permeability nanocrystalline material.

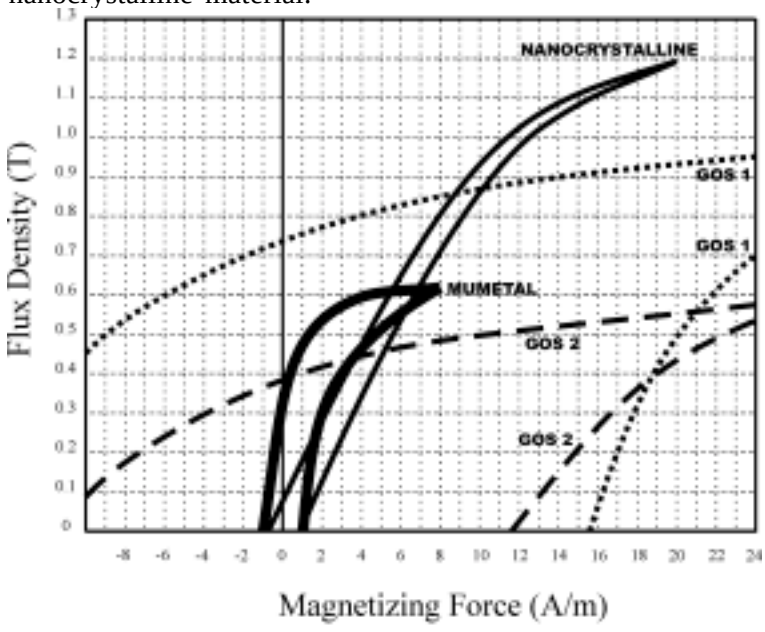

Fig.3 B-H loops for some core materials

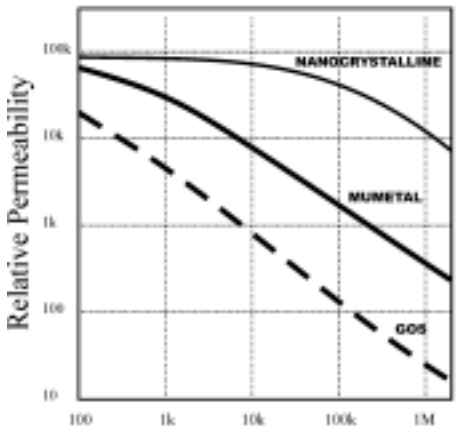

Fig 4 Permeability against frequency

When a ct experiences a primary current pulse there is a tendency for the core to remain magnetised to some extent, a property referred to a remanence. Fig. 3 illustrates this effect. The flux density, B, present in the core once the magnetising force, H, is reduced to zero is a measure of remanence. A high remanence has the effect of temporarily reducing a transformer's I-t capability with successive pulses until eventually a limiting value is reached. It can be seen from Fig 3 that GOS material suffers greatly from this effect, the effect is also noticeable in mumetal but in the nanocrystalline material the effect can be ignored for many practical purposes. The remanent flux density in a core can be reduced to zero or set at a negative value by applying a compensating pulse to the core after the signal of interest has passed. A similar effect can be achieved by the application of an appropriate dc reverse bias current via an auxiliary winding The level of this should be sufficient to reset the core but not so great as to put the core into near reverse saturation.

Application of a resetting pulse can be practical in production equipment where the advantages of lower-cost materials can be exploited. It is less attractive for general laboratory use.

In Fig. 4 the effect of frequency on core permeability is illustrated. Reduction in permeability with frequency reduces L in Figs 1 and 2. This reduced inductance is not of itself a problem as increasing frequency increases the reactance of L to more than compensate for this effect. Low permeability at high frequency, however, greatly increases the flux leakage in the cores. The limitation is most apparent in cores of large diameter. At low frequency the output of a transformer will be found to be independent of the position of the primary conductor. As frequency is increased the position of the primary inductor starts to have an effect on the recorded current waveform. It is this loss of permeability with frequency that effectively limits the use of GOS material. In large transformers that contain distributed windings, sensitivity to stray magnetic fields and primary conductor position can limit performance rather than the effects of parasitic inductance and capacitance. To a lesser extent the effect can also be seen in ct's that utilise cores containing nanocrystalline materials.

PULSE PERFORMANCE OF TWO PULSE TRANSFORMERS EMPLOYING GOS CORES

In Table 1 the performance of two large diameter current transformers is illustrated. These ct's were manufactured with cores made from GOS material. The instruments were terminated externally with an effective value of R_B of 25R. The high-frequency cut-off value was somewhat arbitrarily determined. In both units A and B it was the frequency at which the positioning of the

primary conductor at any point within the central aperture of the toroid caused a 3dB deviation in output from the true reading. The lf cut-off value was the frequency at which the output was 3dB down on the true value. I-t capability with no reset was recorded after the application of several successive 1000A pulses. Reset was achieved by following each pulse with the momentarily application of a 12AT pulse to an auxiliary reset winding.

Table 1
Performance of two externally terminated ct's with GOS cores

Trans-former	Inner Diameter	Afe	Ratio	Sensitivity	Lf cut-off	Hf cut-off	I-t Reset	I-t No reset
	cm	cm^2		V/A	Hz	kHz	As	As
A	13	1.3	3000:1	0.00833	0.2	100	17.4	4.5
B	6	2.7	500:1	0.05	6.0	500	6.0	0.67

The results illustrate that low-cost GOS cores with simple termination can be used to monitor pulse currents where frequency components measured in tens of kilohertz are present. The application of a reset pulse compensates for the material's high remanence. The lf and I-t capabilities of the test pieces could be extended by reducing the value of effective R_B as indicated in Eqs. (1) and (3) with an accompanying reduction in sensitivity.

Internally-terminated transformers of similar size would have greater bandwidth with the upper frequency cut-off point being extended to several megahertz.. I-t capability would be similar to that achieved with the application of a reset pulse, although with a nanocrystalline core the use of a reset pulse would not be necessary.

MEASUREMENT OF HIGH PULSE CURRENTS WITH CASCADED TRANSFORMERS

In some applications it is necessary to monitor current with an instrument that combines a bandwidth that extends well into the megahertz region with an ability to monitor pulses measured in tens of kiloamps. A core with good high-frequency permeability is required and distributed internal termination. A high transformation ratio is attractive, as, in addition to enhancing I-t capability, Eq. (3), it would reduce the current in the measurement resistors R_B. However, a large number of turns dictates that a high number of series-connected stages would be required to satisfy the frequency response demand thus increasing production costs. The number of stages also reduces the resistance value of the individual sense resistors that form R_B so increasing the effect of parasitic inductance L_B in Fig. 2. Under these circumstances there can be some merit in using two cascaded transformers [4] as illustrated in Fig. 5.

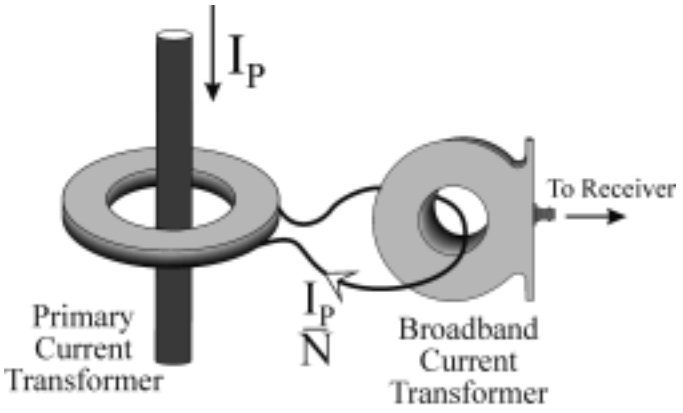

Fig. 5

In this arrangement a relatively simple transformer construction is used to reduce the effective magnitude of primary current whilst preserving its waveshape. This attenuated signal is fed into a standard internally-terminated broadband current transformer for monitoring. It is unlikely that a ratio in excess of 100:1 will be required for the first transformer. The I-t capability of the unit is upheld by ensuring the value of $R_W + R_B$ in Eq. (3) is kept low. R_W is reduced by the appropriate choice of wire and R_B is eliminated. The value of L and its associated low-frequency characteristics are less good than if the system transformation ratio were to be achieved in a single unit although the high-frequency performance is likely to be much better. In this arrangement, low-frequency performance is effectively traded for improved high frequency response.

CONCLUSION

1. The high-frequency performance of broadband current transformers can be limited either by internal parasitic components or the hf permeability of the core material.
2. Cores manufactured from nanocrystalline material can be employed in instruments requiring maximum bandwidth and I-t capability without recourse to reset pulses.
3. Low-cost GOS material core material can be employed in the manufacture of current transformers with bandwidths to several hundred kilohertz.
4. Cascading of transformers can be considered where both high-frequency response is required and high pulse currents are to be measured.

REFERENCES

[1] D.J. Chamund, International Symposium on Pulse Power Applications, Korea, Oct., 2000. p72
[2] M.A. Nadkarni, and S. Ramesh Bhat., 1985, Pulse Transformers - Design and Fabrication, Tata McGraw-Hill Publishing, India
[3] B.V. Cordingley, IEE Conference Publication No.498 (1998) p.433
[4] Elektor Electronics, December, 1994, p100

SOLID STATE THYRATRON REPLACEMENT

A.W. Dunlop, DYNEX Semiconductor, UK

Abstract

This paper describes a solid state alternative to thyratron switching devices. It includes details of the drive electronics and shows a completed prototype assembly. The paper includes a discussion on the choice of appropriate semiconductors for high voltage switching, where the required operating voltages are being achieved by using series connected devices. The techniques used for static and dynamic sharing of voltage across the series stack is also discussed, together with the importance of providing adequate gate drive. Oscillograms showing the effect of gate drive on delay time, rise time and turn-on energy is given, including details of the gate drive circuit used. A photograph of the prototype assembly of the series connected semiconductor switch stack is also shown. Testing of this at the full design voltage has yet to be completed, but results using a voltage scaled equivalent demonstrate that for many applications a solid state switch could offer advantages of low standby power, high average current and longer shot life. Further work is necessary to complete the characterisation of the assembly. Future work could make use of semiconductors that have the ability to turn off, thereby reducing or eliminating PFN components.

KLYSTRON OPERATION STATISTICS AT KEK ELECTRON/POSITRON INJECTOR LINAC

Tetsuo Shidara and KEK Electron/Positron Injector Linac Group
KEK, Oho, Tsukuba, Ibaraki 305-0801, Japan

Abstract
The KEK electron/positron injector linac is supplying 8 GeV electron beams to the KEKB high-energy ring and 3.5 GeV positron beams to the low-energy ring, as well as 2.5 GeV electron beams to the PF and PF-AR rings. This linac comprises a special accelerator module that includes a bunching section and 56 regular accelerator modules, each involves a 40 MW rf source with SLED and four 2-m accelerator sections operated at 2856 MHz. The operation time of the KEKB linac will amount to 7200 hours for fiscal year 2000 because of the heavy competition with the PEPB. More than 100 50-MW klystrons have been produced. Their average life time and MTBF value reached 13500 and 70500 hours, respectively, which shows an affirmative insight into achieving a desirable average life time of 30000 hours.

KEK ELECTRON/POSITRON INJECTOR LINAC

The KEK electron/positron injector linac was originally designed to provide 2.5 GeV beams to both the Photon Factory (PF) storage ring [1-2] and the TRISTAN accumulator ring (PF-AR). The linac upgrade for the KEK B-Factory [3] was carried out since 1994, while always keeping beam injection to the PF and PF-AR rings, and finished upgrading by May, 1998.

The major differences between the upgraded and old injectors are listed in Table 1.

Table 1
Differences between the upgraded and old injectors

	Old	**Upgraded**
Total energy	2.5 GeV	8 GeV
Linac length	400 m	600 m
Accelerator modules	41	59
Energy gain	8 MeV/m	20 MeV/m
Pulse structure	multi-bunch	single-bunch
Pulse repetition	50 pulse/s	50 pulse/s
Positron intensity	0.032 nC/pulse	0.64 nC/bunch

An 8 GeV beam can be provided by accelerating electrons along the entire linac length. In the 3.5 GeV positron-injection mode, a tungsten target is inserted into the beam line at the middle part of the linac; a high-current beam hits the target and part of emerged positrons is accelerated in the remaining part of the linac.

The electron source for the 2.5 GeV electrons to PF and PF-AR still remains at the original part of the old injector.

The upgraded injector comprises a special accelerator module that includes a bunching section and 56 regular accelerator modules, each involves a 40 MW rf source with SLED and four 2-m

accelerator sections operated at 2856 MHz.

50 MW KLYSTRON

A 50 MW klystron was developed for new rf system [4-5], expecting an enough margin at 40 MW operation. The specifications of the 50 MW klystron are shown in Table 2.

Table 2
Specifications of the 50 MW klystron

Beam voltage (kV)	304
Beam current (A)	352
Microperveance	2.1+-0.1
Beam pulse width (μs)	6
rf pulse width (μs)	6
rf top pulse width (μs)	4
Pulse repetition rate (pps)	100
rf frequency (MHz)	2856
Peak output power (MW)	50
Efficiency (%)	45
Gain (dB)	53
Focusing magnet	electromagnet
Pulse transformer step-up ratio	1 : 13.5

OPERATION STATISTICS

The operation time for the KEK electron/positron injector linac is shown in Table 3. It had increased to 7000 hours during FY 1999 due to the start of the KEKB experiment and will amount to 7200 hours for FY 2000 because of its heavy competition with the PEPB.

Table 3
Operation and failure rate

Period (FY)	**Operation time (hours)**	**Failure rate (%)**
1993	5299	0.88
1994	5070	0.78
1995	4563	0.74
1996	4123	0.62
1997	3828	2.88
1998	5906	7.12
1999	7297	7.36
2000	7160	

The cumulative klystron operation status up to March 2000 is shown in Table 4. More than 100 50-MW klystrons have been produced. Their average life time and MTBF value reached 13500 and 70500 hours, respectively, which shows an affirmative insight into achieving a desirable average life time of 30000 hours.

Table 4
Cumulative klystron operation status up to March 2000

Fiscal year of product	Total No. of tubes	Unused No. of tubes	Living		Failed		Cumulative operation (tube-hrs)	MTBF (hrs)
			No. of tubes	Av. op. time (hrs)	No. of tubes	mean age (hrs)		
1993	14	2	10	19184	2	20188	232212	116106
1994	13	0	11	17624	2	5857	205580	102790
1995	23	0	15	16212	8	7191	300705	37588
1996	15	0	12	14326	3	6707	192031	64010
1998	20	1	19	6668	0		126684	
1999	15	14	1	1884	0		1884	
total	100	17	68	13667	15	8649	1059096	70606

References

[1] J. Tanaka, Nucl. Instr. and Meth., 177(1980)101.

[2] I. Sato, Nucl. Instr. and Meth., 177(1980)91.

[3] A. Enomoto, et al., Proc. of the 1993 Particle Accelerator Conference, U.S.A., 1993.

[4] S. Anami et al., Proc. of the 1993 Particle Accelerator Conference, U.S.A., 1993.

[5] S. Fukuda et al., Proc. of the 1994 Linear Accelerator Conference, Japan, 1994.

FIM TECHNOLOGY

Claude VINCENT
TPC / Avenue du Colonel Prat / 21850 St. Apollinaire / France

INTRODUCTION

For more than 30 years, energy storage capacitors have been designed according to the existing technologies used in filter capacitors. The dielectric, including insulating layers and impregnant have been mainly adapted to the specificities of discharge application conditions. This was particularly significant in the 90's, during which a profound change of d.c. filter capacitor technology led to a new line of energy storage capacitors based on an all film design, which integrated all the knowledge acquired, not only in the d.c., but also in the a.c. field.

D.C. CAPACITOR EVOLUTION

In 1960, the usual design of d.c. filter capacitors for medium and high voltage, based on a mix of paper + aluminium foil impregnated with mineral oil, was improved when replacing the mineral by castor oil.

In 1970 when polypropylene film appeared, the dielectric was modified : the mixed dielectric (paper and film) was impregnated with a synthetic oil, but the energy density did not increase significantly. All-paper designs remain the reference in many large projects.

In the meantime, for voltages ranging from 900 volts up to 5000 volts, metallized paper is an interesting solution, especially in terms of controlled lifetime.

Used with one or two layers of paper, or with a polymer film, it has become the reference for filter and energy storage capacitor, mainly because the self-healing properties of the metallization.

During this long period, a lot of improvements have been carried out with respect to:

- the performance of paper (density increased up to 1.35 - number of weak points reduced)
- the edges of aluminium layers (laser cut to avoid sharp edges)
- the manufacturing process (better control of paper drying by measuring the depolymerisation index)

However two major points limit the performance of these capacitors:

- aluminium foil capacitors: no information can prevent against the breakdown and/or the short circuit
- metallized paper capacitors: the self-healing properties of metallized film capacitors induce large quantities of gases, which increase the internal pressure. Protective devices like pressure switches and/or disconnectors (for filter capacitors) try to limit the negative effect of the gas, but at the end of life, there is still a large amount of bulging on the sides of the can.

At the end of the 80's, this situation was no longer acceptable for the traction field, using very large capacitors banks. It became necessary to create some fundamental changes in the capacitor design.

NEW REQUIREMENTS

For new traction projects, which started in 1990, new specifications appeared based on two keywords : safety and control.

The main criteria for the D.C. capacitors were :

- completely safe products (no explosion or catastrophic failure)
- capacitance control over the lifetime of the device
- no bulging of the can
- high power available
- reduced weight and volume
- high tolerance of peak discharge currents

Quite the same requirements appeared for energy storage capacitors devoted to electric guns and large laser projects.

A wide program of development was launched in 1989, with two main ideas:

- the dielectric must be a polymer
- the metallization must participate to a better use of the dielectric

THE NEW D.C. CAPACITOR

A choice of the most accurate combination of raw materials was made from a group of three polymers, three metallization types and eight impregnants. Considerations for this choice included chemical and physical test files, like compatibility between the components, and electrical tests including:

- 32 hours step stress tests to reach the dielectric limits
- long time (500 to 10000 hours) endurance tests at high temperature (70°C)
- Discharge tests to simulate faulty working conditions.

All these electrical tests were performed on industrial size windings or capacitors.

The best combination was an association of **polypropylene film**, **aluminium metallization** with reinforced edges and **rapeseed oil**.

Raw materials

The polypropylene film

This film met practically all the requirements needed by the D.C. capacitors.

- available thickness between 4 and 20 microns
- Surface roughness from 0.02 µ (smooth film) up to 2 µ (rough film also called hazy film)
- low number of conductive points : average of 0.4/ m² under 300 v/µ
- dielectric constant lower than hoped : 2.2
- high level of electrical breakdown. Fig 1 shows the minimum, maximum average breakdown values

depending on the thickness of the film for one manufacturer.

- high level of reliability and repetitivity of the film batches.

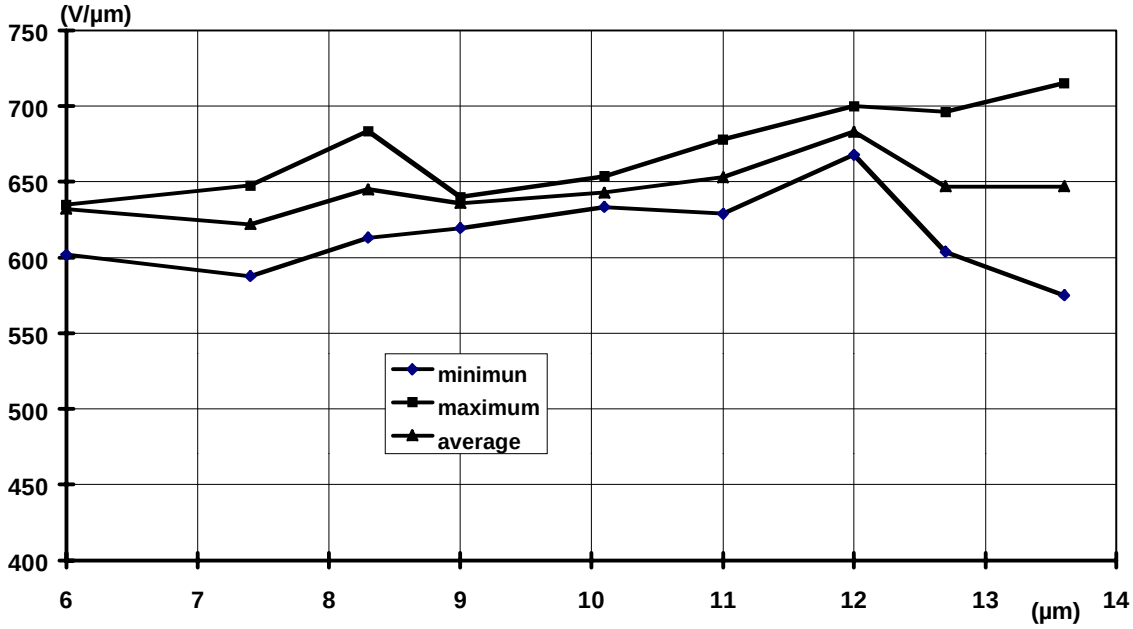

Fig 1 Dielectric strength on hazy polypropylen film vs thickness

Metallization

The metallization is the key to the self-healing process. It can be altered or adjusted in several ways in order to minimise this process, for instance, by surface segmentation or with various resistivities ,or multi-tracks designs which help increase the voltage of the winding.

When the surface is segmented (see drawing hereunder), generally fuses protect small areas. When a puncture occurs in one area, the fuse is blown out and the corresponding area is insulated , leading to a reduced capacitance loss.

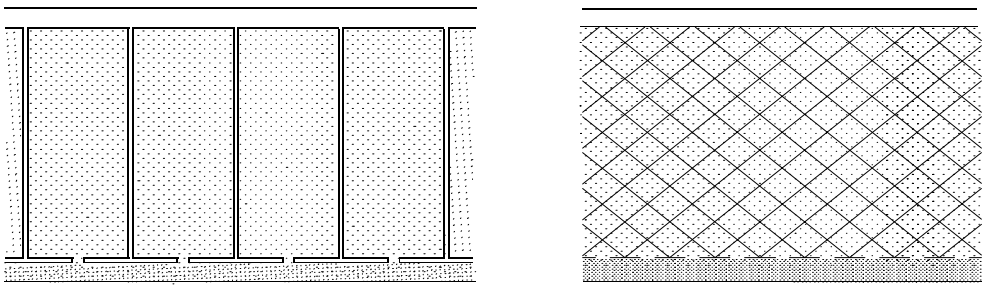

Hereafter are summarised some results regarding the influence of segmentation over a 6 years period:

Year	1990	1992	1994	1996	2000
Segmentation	T	T	Mosaic	T	sprayed
Surface unit (cm^2)	42	42	1	28	0.00001
Fuse / unit	1	1	4	1	1
Stress	1	1.1	1.33	1.47	1.67
Volume	1	0.79	0.54	0.36	0.29
Weight	1.35	1.07	0.73	0.49	0.39

Without any segmentation, the goal is always to obtain a small demetallized area around the puncture of the film sufficient to withstand the applied voltage without any secondary effect on the closed layers, despite the surrounding energy.

The rape seed oil

In addition to the usual requirements, like reliability and homogeneity between batches, rape seed oil presents two main performances:

- Due to its low viscosity, it flows easily between the film layers during the filling operation. It impregnates the film, but only slightly because of its permachor value so that the swelling of the film does not exceed 2 to 2.5%.This avoids having any effect on the behaviour of the metallization on the film.
- High gassing property, probably one of the best among the impregnants, allows it to work under the worst conditions of partial discharges. The gas bubbles which occur at each shot (in case of surge voltage in the filter capacitor) are absorbed by the liquid.

In addition, its high flash point (250 °C) and fire point (300 °C) make it comparable to castor oil.

Properties of the capacitor

The initial requirements for safety have been fulfilled: no remaining short circuit. Only a drop in capacitance due to the fuse effect or the demetallized area is evident. At the end of filter capacitor life, the drop in capacitance is 2% (typical value) without any bulging of the can. For energy storage capacitors, this capacitance drop can reach 5% of the initial value, depending on the customer's specifications.

Fig 2 shows a test result obtained when testing a 30 liters capacitor at 1.8 times its nominal voltage. At the end of the test, the whole capacitance is lost and the swelling of the can is limited to an acceptable width. With a capacitance lost of 2%, i.e. at the real end of life, no bulging occurs.

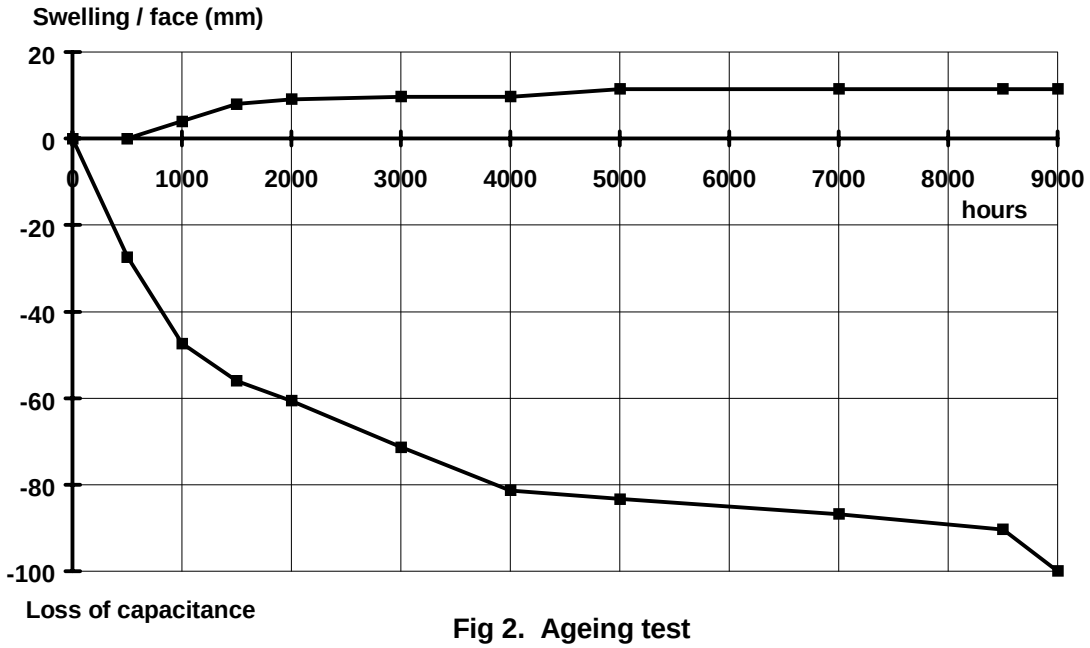

Fig 2. Ageing test

- volume and weight : compared to the 1990 situation, to date, volume in divided by 3.7 and the weight by 3.1.

These two large reductions are a result of the constant increase of the dielectric stress and the replacement of paper (density : 1.35) by polypropylene film density : 0.9). Consequently, the density of the capacitor drops from 1.65 down to 1.25.

Capacitance control

In most applications, capacitance control, operated according to the control plan of the user, can be used to indicate ageing of the component. This makes prediction of capacitor replacement possible because no failure is observed.

When a problem is detected, for example an unacceptable drop in capacitance or increase of loss factor., an analysis of the capacitor could reveal the reason for the observed deviation.

The capacitor in this case acts as a detector. If there is a large number of self-healing points and corresponding blown fuses, the capacitor is being subjected to unexpected high surge voltages.

If , there is a normal number of self-healings points and a large number of blown fuses, high currents are going through the capacitor.

If the contacts between metallization and metal spraying are crowded, surge currents exist in the loop where the capacitor is installed.

Experience

Over the ten last years, about 54 000 capacitors based on the above design have been operating in the field without any defects. The Mean Time Between Failure resulting from this experience is now more than 10,000 million hours.

TRANSFER TO ENERGY STORAGE

Because of the positive results presented by this technology and the high performance obtained in the short term endurance tests, a new development started in 1995.

The working parameters are totally different to those of filter applications. It is therefore necessary to study two main fields :

- behaviour of the dielectric under high stress
- influence of the reversal voltage, the hold time at full voltage, the charging time and the repetition rate

Dielectric stress

Even if the drop in capacitance is extended to 5% at the end of the life of the capacitor, the objective is to reduce the drop in individual capacitance to a minimum value.

The initial "T" segmentation pattern created a 42 cm^2 elementary capacitance surface. The mosaic solution is not completely adapted to large discharge currents.

To date, the solution is based on the association of two effects. The first one is the self-healing itself, which will complete its process once initiated. In case of trouble, a second level of safety is provided by the remaining fuses.

At first, the drop in capacitance is equivalent to some mm^2. The fuses then insulate some cm^2.

With this solution, the drop of capacitance is strongly reduced, placing it totally with a secured process.

Reversal voltage

As observed in the filter capacitor working under faulty conditions, mainly in case of an external short circuit, the reversal level leads to important modifications in the lifetime of the capacitor.

Fig 3 shows the results of tests performed on medium size capacitors which are subjected to a 1000 shots-per-step test. Between 10 and 90% reversal, the ratio of the volume for the same lifetime is about 2.

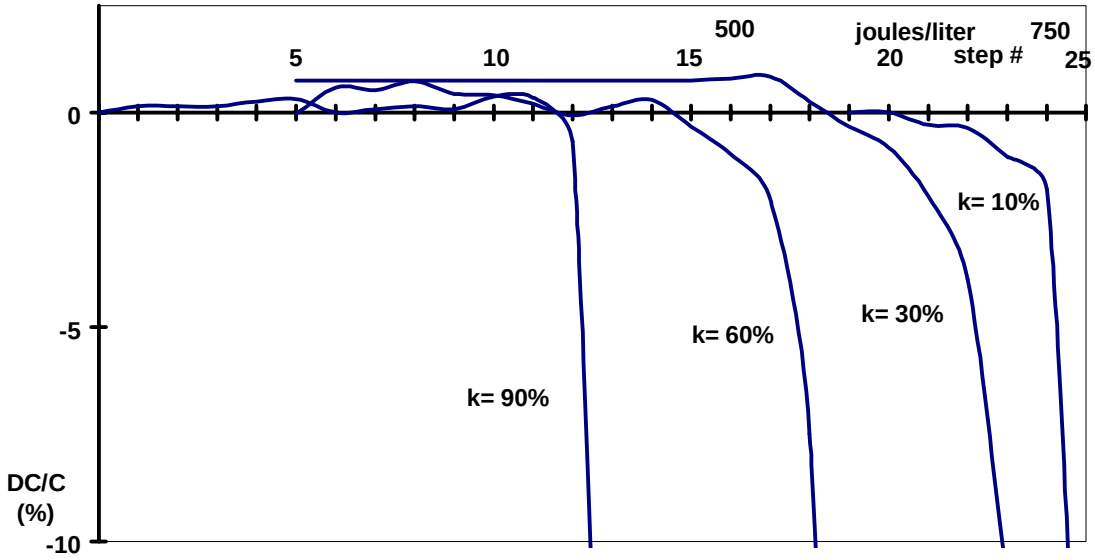

Fig 3. Capacitance drop vs 1000 shots/step

Thanks to the design of these units, the curves are very precise (the distribution is well centred), compared to those which are found in the paper/film/aluminium foil technologies.

Also, for high voltage reversal, the ageing of the capacitor becomes significant.

Fig. 4 shows a test result reached under the following conditions : 10 000 shots with a 10% voltage reversal, followed by 25 shots at 60% voltage reversal and again by 10,000shots under the initial conditions.

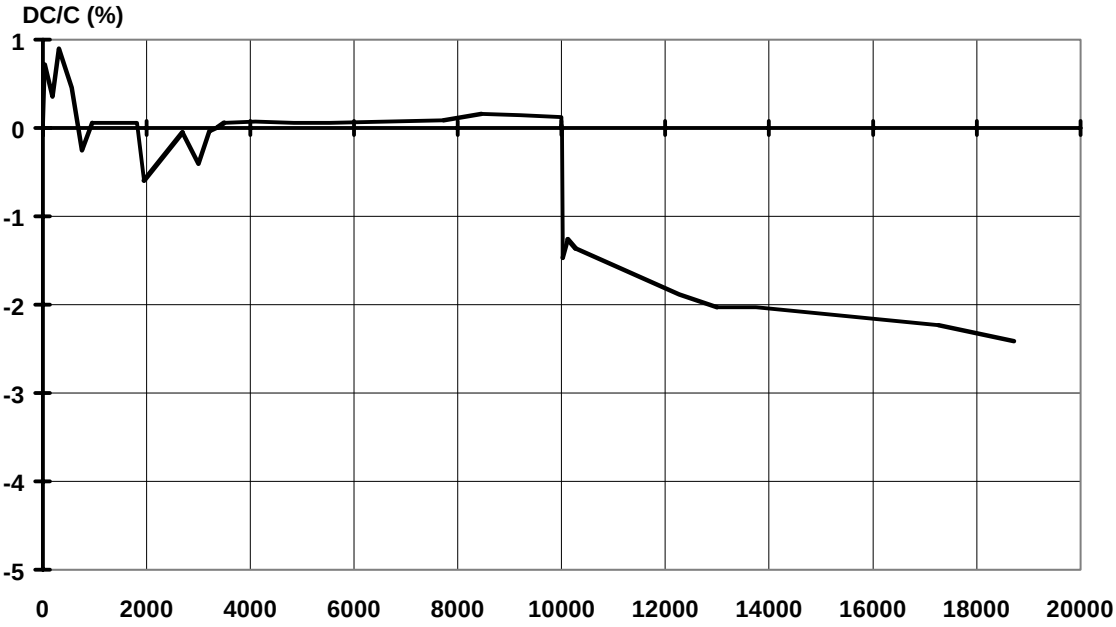

Fig 4 Capacitance vs # shots (10% reversal + 25 shots at 60%)

In the first period no change of the capacitance occurs. The next 25 shots lead to a significant, but controlled decrease of the capacitance (practically the same value per shot). In the last period the capacitance is decreasing slowly, because the film has aged after the 60% reversal voltage test.

CONCLUSIONS

The first objective: the safety characteristic of metallized (**M**) polypropylene film (**F**) impregnated (**I**) with rape seed oil (**FIM technology**), is reached. Due to technology improvement, we multiplied by 3 the energy density for D.C. filtering and now for energy storage field. The maintenance is light due to only capacitance and loss factor measurements. This technology is replacing the previous film foil capacitors.

Modular Solid-State Switch for the SPS and LHC Beam Dump Systems

J. Bonthond, L. Ducimetière, P. Faure, E.B. Vossenberg
CERN, Geneva, Switzerland

Abstract

A modular coaxial solid-state closing switch has been developed for the physical replacement of a NL488A high-density graphite anode, water-cooled ignition in the horizontal sweeper generator of the beam dump system of the CERN SPS accelerator. The main reasons for the development in this application were environmental, low maintenance and exclusion of erratic firings. Two prototype switches have been made for a hold-off voltage of 12 kV. They consist each of a stack of four asymmetrical Fast High Current Thyristors together with capacitive over-voltage protections and resistive dividers. A specially designed trigger transformer allows the reuse of the original ignitron trigger unit without modification. The switches conduct a 46 μs half sine wave peak current of 25 kA at an initial rate of 2 kA/μs. Their losses are about 80 Joules per discharge at 12 kV. The minimum repetition rate is 5 seconds. The two switches have successfully operated for one year and the series is now under installation.

A similar switch has been designed for the LHC beam extraction system to prevent erratic firings. It consists of 10 series connected asymmetrical FHCT's and its total stray inductance is less than 150 nH. It has a hold-off voltage of 30 kV and switches a peak current of 20 kA in less than 2.7 μs. The 10:1 trigger transformer has a 5 μH stray inductance, which allows, at 2 kV primary trigger voltage, a peak gate current of 250 A with a rate of rise of 400 A/μs. This switch has been tested over several years and has already demonstrated some 300.000 shots without any break-down or erratic firing. The test repetition rate of the switch varies between 8 hours and 20 seconds.

For reliability and standardization reasons, this switch will also be used in the pulse generators for the horizontally and vertically deflecting diluter systems of the LHC beam dumping system. The particularity of the switch for the horizontal system is the fact that its current is an attenuated sinusoidal oscillation of 25 kA amplitude at a frequency of 14 kHz. Tests have shown that, due to the lifetime constant of the charge carriers of about 500 μs, no anti-parallel diodes are required for the reverse current in the FHCT's.

Introduction

Horizontal Sweeper Generator Beam Dump system SPS (MKDH)

The horizontal beam dump system uses 3 fast kicker magnets per beam to deflect horizontally the particles in one revolution of the accelerator on an absorber block, which is located in the SPS tunnel. Each kicker magnet is powered by two pulse generators, which are connected in parallel. They consist of a discharge capacitor, a resistive crowbar circuit and a switch, that produces at 12 kV a magnet current pulse of 25 kA amplitude of 25 μs rise time and 120 μs fall time. The magnet current has to be proportional to the beam energy over a dynamic range of 30, from injection at 15 GeV/c to a top energy of 450 GeV/c. During a SPS machine cycle of 14 seconds the horizontal sweeper generators are constantly under a voltage of 10 kV.

As new power switches, semiconductor solid state technology has been chosen to assure the absence of erratic firing.

Beam Extraction system LHC (MKD)

The beam extraction system uses 14 fast kicker magnets per beam to deflect horizontally the particles in one revolution of the collider in an extraction channel and after being diluted the beam is disposed on external absorbers blocks, which are located at the end of tunnels excavated roughly tangentially to the LHC ring. Each extraction kicker magnet is powered by its own pulse generator, which consists of a discharge capacitor and a semiconductor solid state switch, that produces a magnet current pulse of 20 kA amplitude of

2.7 µs rise time and 90 µs flattop. The magnet current needs to be proportional to the beam momentum over a wide dynamic range, from injection at 450 GeV/c to a top momentum of 7 TeV/c. During a collider run of e.g. 6h the beam extraction generators are continuously under a voltage of 30 kV.

Also here semiconductor solid state technology has been chosen for the power switches to assure a high level of reliability and availability and the absence of erratic firing. A fault tolerant re-trigger system will be installed that triggers all the switches in case of a spontaneous discharge in one of the generators.

Dilution system of extracted LHC beam (MKB)

Each extracted beam is diluted upstream the extraction tunnel by a set of orthogonally deflecting kicker magnets. They consist of four horizontally and six vertically deflecting systems. Each system includes a high voltage generator capable to power the corresponding magnet with an attenuated high current sine wave of over 25 kA amplitude at a frequency of about 14 kHz. The magnet current phase shift between the horizontally and vertically deflecting systems is 90 degrees. Each high voltage generator consists of a discharge capacitor and a semiconductor solid-state switch. After the extracted beam has been deflected by the diluter magnets it produces after 650 m at the end of the extraction tunnel an ♏-form like sweep with a radius of 35 cm on the front surface of the beam dump block. In this application the magnet current is also proportional to the beam momentum like for the MKD magnet.

Switch requirements

MKDH

The basic circuit diagram of the MKDH generator, the 12 kV switches (Swa and SWb) and the circuit diagram of the switch are shown in Fig. 1 and Fig. 2. Fig. 3 shows the installed switch in the MKDH generator and Fig. 4 shows the current waveform at 12 kV. The switch requirements are indicated in Table 1.

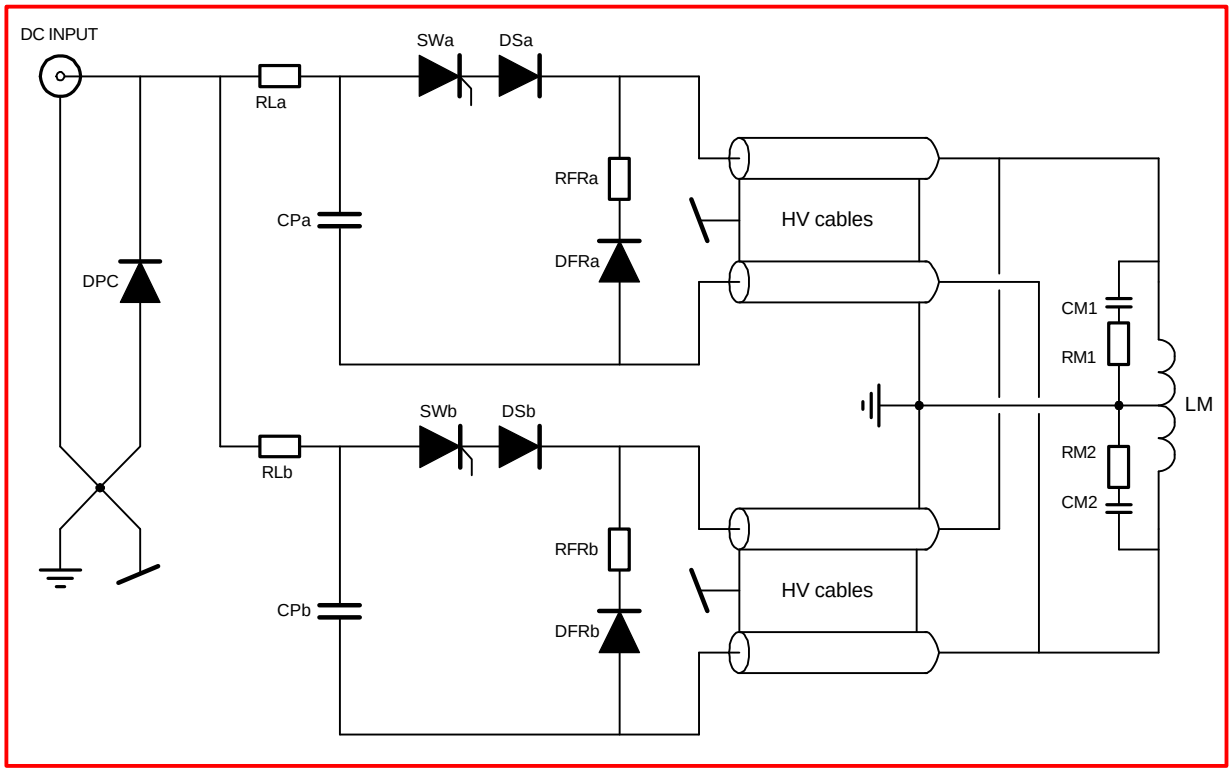

Fig. 1: Basic circuit diagram of MKDH generator

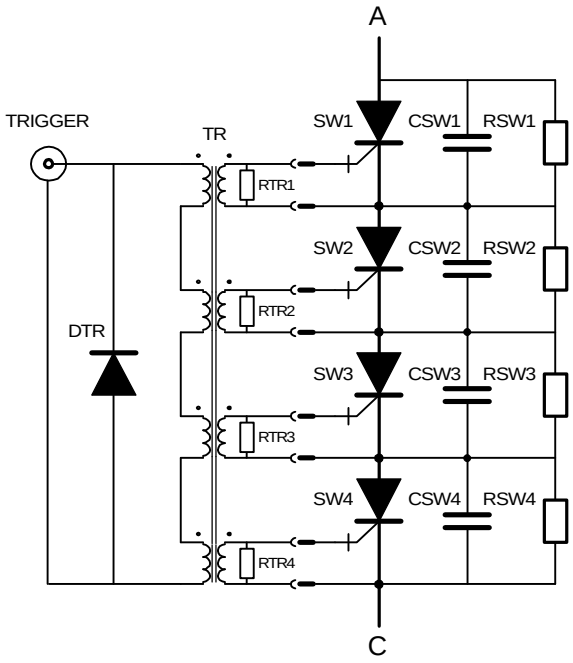

Fig. 2: Circuit diagram of MKDH switch

Fig. 3: Installed MKDH switch

D.C. operating voltage range	330-10000	V
Current amplitude	690-21000	A
Current rise/fall time	23/23	µs
Current max rate of rise/fall	2/1.5	kA/µs
Current pulse duration	46	µs
Charge transfer	780	mC
Max. switch conduction losses	82	J
Repetition time min. @ 12 kV	5	s
Repetition time typ. @ 10 kV	14	s
Total lifetime	2000000	pulses
Prefire rate	$< 10^{-4}$	

Table 1: MKDH switch requirements

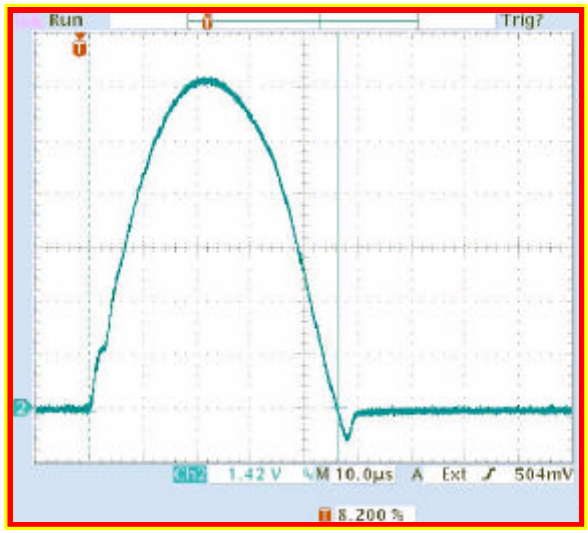

Fig. 4: MKDH switch current at 12 kV
(Hor. scale 10 µs/div., Vert. scale 4 kA/div.)

MKD

The basic circuit diagram of the LHC Beam Extraction generator is shown in Fig. 5. Four 30 kV switches for the LHC beam extraction system have been assembled. The switch is composed of ten asymmetric 4.5 kV thin wafer FHCT's. Anti-parallel diodes are not employed in the switch. In order to safely operate the FHCT's in series with a small spread in turn-on time, gate currents are employed with a high amplitude and high rate of rise. Measurements on the prototype 30 kV switch assembly showed a maximum spread in turn-on time of less than 50 ns. Protection of the FHCT's against over-voltages caused by differences in switching speed and turn-on delay, is realised by capacitors connected in parallel to the FHCT's. The value of these capacitors is kept to a minimum so that they not only protect against over-voltage but also improve the turn-on time by internal discharge over the FHCT's during turning on.

The circuit diagram of the switch is shown in Fig. 6. The measured current of the MKD switch and switch requirements are indicated in Fig. 7 and Table 2.

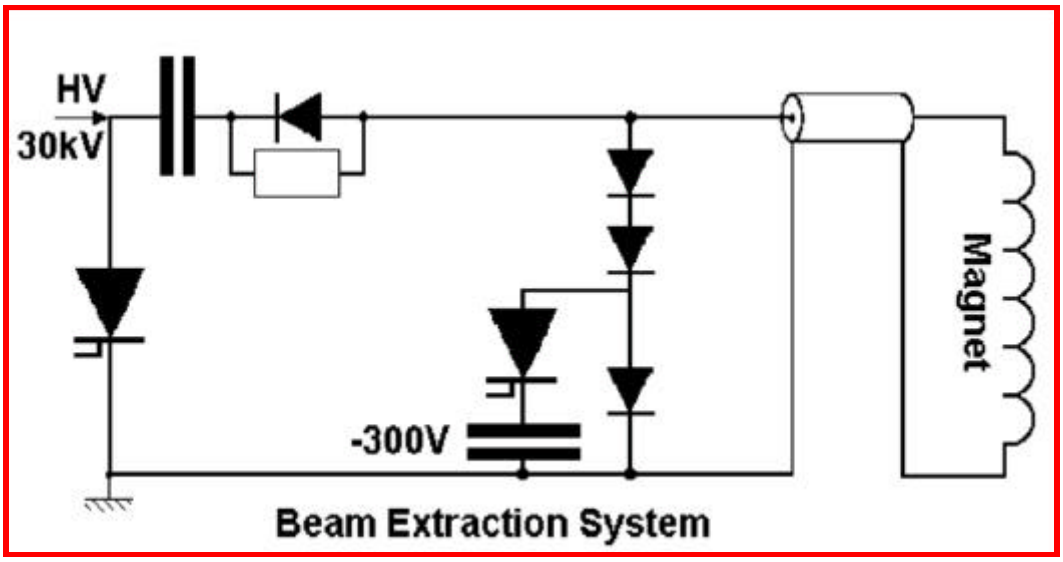

Fig. 5: Basic circuit diagram of MKD generator

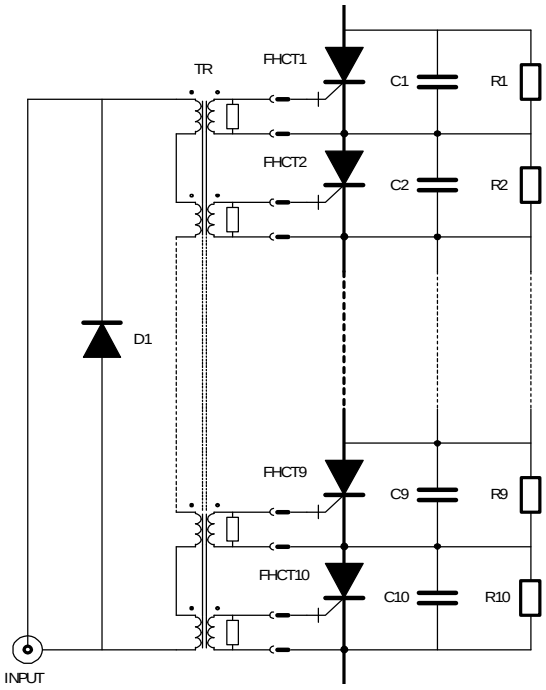

Fig. 6: Circuit diagram of MKD switch

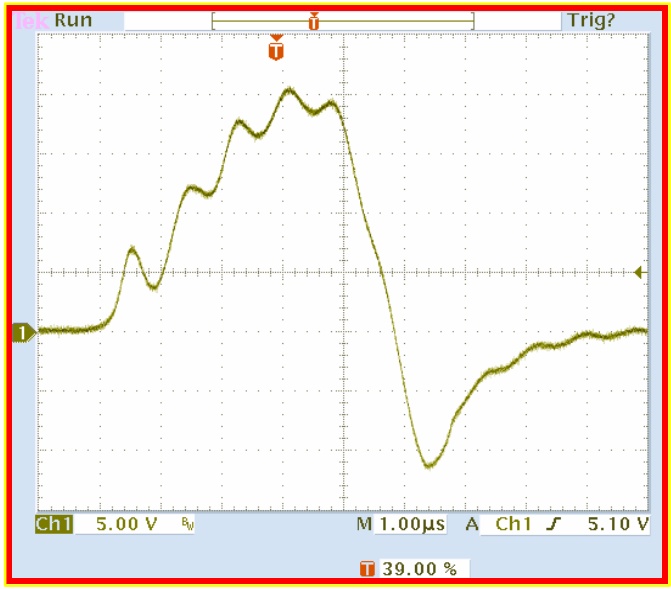

Fig. 7: MKD switch current at 30 kV
(Hor. scale 1 µs/div., Vert. scale 5 kA/div.)

D.C. voltage range	3-30	kV
Max current amplitude pos./neg.	+20/-10	kA
Current rise/fall time	2.75/1.5	µs
Max. current rate of rise/fall	15/20	kA/µs
Current pulse duration pos. + neg.	8	µs
Charge transfer pos./neg.	59/17	mC
Max. switch conduction losses	12	J
Repetition time min. @ 30 kV (test)	20	s
Repetition time typ. @ 30 kV	6	h
Total lifetime	500000	pulses
Prefire rate	$< 10^{-4}$	

Table 2: MKD switch requirements

MKB

The basic circuit diagrams of the LHC Beam Diluter generators are shown in Fig. 8. There are two type of diluter systems: horizontal and vertical. The switch for both systems is similar to the MKD switch. Measurements on a single asymmetric 4.5 kV device showed that in case of the horizontal diluter generator, a damped oscillating switch current of 30 kA, shown in Fig. 9 does not impose anti-parallel diodes for the reliability of the FHCT stack. The switch requirements are indicated in Table 3.

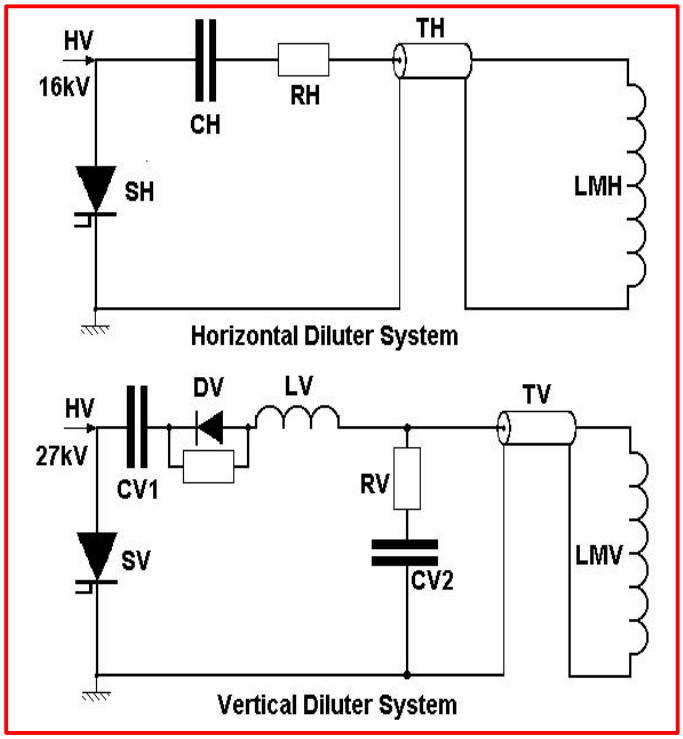

Fig. 8: Basic circuit diagram of MKB generators

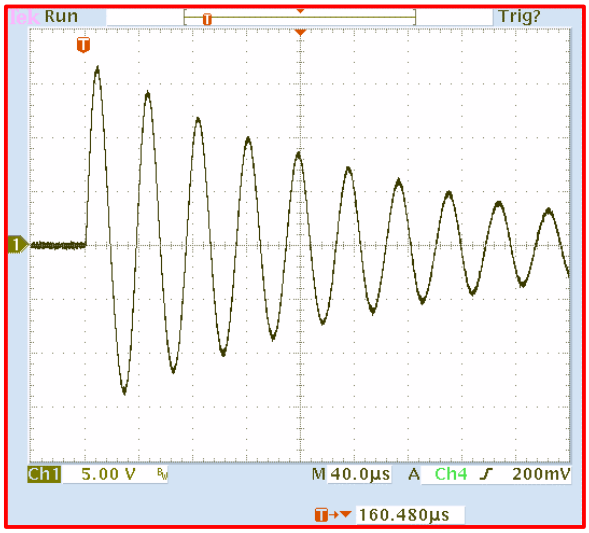

Fig. 9: MKBH test switch current (32 kA)
(Hor. scale 40 µs/div., Vert. scale 10 kA/div.)

D.C. voltage operating range	3-27	kV
Max current amplitude pos./neg.	+25/-22	kA
Current rise/fall time	18/18	µs
Max. current rate of rise/fall	4/4	kA/µs
Current pulse duration	500	µs
Charge transfer pos. + neg.	4.8	C
Max. switch conduction losses	608	J
Repetition time min. @ 30 kV (test)	20	s
Repetition time typ. @ 30 kV	6	h
Total lifetime	500000	pulses
Prefire rate	$< 10^{-4}$	

Table 3: MKB switch requirements

Conclusion

FHCT's with large junction sizes are capable of fast switching high currents. Elements of 4.5 kV can operate as closing switches with a di/dt of 20 kA/µs and peak currents of tens of kiloamps. The life time carrier control and the gate drive power supplies must be optimised for each application. Successful operation of a modular solid state switch has been demonstrated. The switches have been operated at room temperature and at relatively low repetition rates.

Due to the soft turn-on, noise levels are kept to a minimum. For high voltage applications, series connected FHCT's can probably in certain cases replace gas and vacuum switches. Parallel capacitor arrangement can accommodate mismatches in switching speeds of the FHCT's and ensure a satisfactory over-voltage protection during turn-on. The testing of solid state switches in the three applications will start later this year.

References

[1] J. Bonthond, L. Ducimetière, G. Schröder, E. Vossenberg of the LHC Beam Dump System, "A High Current Sinusoidal Pulse Generator for the Diluter Magnets", Proc. 24th International Power Modulator Symposium, 2000.

[2] L. Ducimetière, G. Schröder, E. Vossenberg, "Improved Turn-on Characteristics of Fast High Current Thyristors", Proc. 23rd International Power Modulator Symposium, 1998.

[3] E. Carlier, L. Ducimetière, U. Jansson, M. Schlaug, G. Schröder, E. Vossenberg, "Solid State Switch Application for the LHC Extraction Kicker Pulse Generator", Proc. 22nd International Power Modulator Symposium, 1996.

[4] J. Bonthond, L. Ducimetiere, G. Schröder, E. Vossenberg, WESTCODE, "High current, high di/dt switching with optimised GTO thyristors", Proc. 21st International Power Modulator Symposium, 1994.